Specific-heat study of nanocrystalline palladium

Y. Y. Chen
Institute of Physics, Academia Sinica, Taipei, Taiwan, Republic of China
and Department of Physics, Soochow University, Taipei, Taiwan, Republic of China

Y. D. Yao
Institute of Physics, Academia Sinica, Taipei, Taiwan, Republic of China
and Department of Physics, National Chung University, Chiayi, Taiwan, Republic of China

S. S. Hsiao
Department of Physics, Soochow University, Taipei, Taiwan, Republic of China

S. U. Jen and B. T. Lin
Institute of Physics, Academia Sinica, Taipei, Taiwan, Republic of China

H. M. Lin and C. Y. Tung
Department of Material Science, Tatung Institute, Taipei, Taiwan, Republic of China
(Received 24 January 1995; revised manuscript received 16 May 1995)

We have performed measurements of the low-temperature specific heat for $T=0.7$–20 K and magnetic susceptibility for $T=1.8$–300 K of Pd nanocrystals with average particle size 84 Å. An enhancement of the specific heat is observed at temperatures $T>3.5$ K for 84-Å Pd nanocrystals. This enhancement is primarily related to the softening of and the size effect on the phonons. The temperature coefficient of specific heat γ decreases to a lower value as compared to that of bulk Pd. An estimated surface coefficient of specific heat γ_s is about 30% that of the bulk. This is also reflected in a reduction of the magnetic susceptibility of the Pd nanocrystals. The peak of the magnetic susceptibility observed at ~ 80 K in bulk Pd is not observed in the nanocrystals; this could be due to a change of the energy band structure in the Pd nanocrystals.

I. INTRODUCTION

Nanocrystals have been widely studied by scientists in the last two decades because of their unusual structures and the presence of size effects on lattice phonons and conduction electrons.[1–5] Key properties of the nanocrystalline state—higher diffusivity and reactivity, greater ductility, larger thermal expansion, enhanced phonon specific heat, and a significant change in the magnetic susceptibility relative to the bulk—have captured the attention of scientists and engineers because of their potential applications.[6,7] Although a variety of physical properties of nonocrystalline materials have been extensively studied, with an eye to engineering applications, the thermodynamic properties have received less attention. Especially because of the lack of data in the low-temperature region, a systematic analysis on nonocrystals is not easy to achieve. Usually the size of a nanocrystal is on the order of a few tens of angstroms to a few hundred angstroms. This exceptionally small size creates two exotic properties, which are not easily observed in bulk materials. The first is the quantum size effects on the lattice phonons and conduction electrons, which are revealed in thermodynamic properties such as specific heat and magnetic susceptibility. Second, the surface volume fraction is dramatically increased, which makes it possible to study the macroscopic surface physics via thermodynamics. For example, for a spherical nanocrystal with a diameter of 5 mm and an atom size of 5 Å, the surface volume fraction is 6×10^{-4}, but for a nanocrystal with a diameter of 50 Å the surface volume fraction is as large as 6×10^{-1}, which is three orders of magnitude larger than in the former case. In contrast to the oldest work, where nanocrystals were most often formed by thermal evaporation of a film onto a substrate with a low degree of dispersion[8] or were produced by forcing molten metal into porous glass,[9] more recently nanocrystals are typically synthesized in inert gases by means of quick gas condensation. No matter which method is employed, there is an unavoidable creation of some level of micrograins, defects, disorder, oxidation, and intergrain boundaries in nanocrystals for different materials,[10] and, if the effects of these cannot be clearly separated, the thermodynamic and magnetic properties become very difficult to study. A typical example of this is reported in our recent study of the specific heat of copper nanocrystals.[11] For the current study we have obtained better-quality samples of Pd nanocrystals with an average particle size of about 84 Å. Since fewer side effects, such as micrograins, defects, disorder, and intergrain boundaries, appear in these samples, our low-temperature specific-heat measurement shows differences from that of the early work of Comsa, Heitkamp, and Rade.[12] With the advantage of the availability of more work on nanocrystals in the literature, we are in a better position to understand the data for Pd nanocrystals.

II. EXPERIMENTAL DETAILS

To measure the specific heat of bulk Pd, two segments of 2×2-mm^2 cross section and 0.8-mm thickness were cut from an ingot of palladium metal of 99.99% purity obtained from Electronic Space Products International. The Pd nanocrystal powders with an average size of about 84 Å were fabricated on a liquid-nitrogen-cooled cold trap by thermal evaporation in He atmospheres of 100 torr; these were compressed into 20-mg pellets with a diameter of about 2 mm. In Fig. 1 the distribution of particle sizes obtained by transmission electron microscopy for Pd nanocrystals before compression is shown. In order to examine the possible effect of surface oxidation and to determine the structure of the Pd nanocrystals, high-resolution transmission electron microscopy was performed on the same batch of Pd nanocrystals; an example is shown in Fig. 2. In this figure no abnormal lattice spacing at the rim of the nanocrystal was observed (in the case of oxidation a different lattice spacing will be seen because of the lower density of oxidized Pd—for instance, the lattice constant of PdO is 5.65 Å); this indicated that at least no remarkable oxidation occurred on the surface of nanocrystal. Auger spectroscopy of the specimen did show very little trace of oxygen, which may come from the absorbed oxygen on the surface of Pd nanocrystals.[13] One indication of no excessive oxidation on the surface of Pd nanocrystals was that, after the nanocrystals were pressed into pellets, the surface of the pellets exhibited Pd metallic reflection with no sign of oxidation. To examine the effect of reduction on the specimen, the specimen was stored in a hydrogen atmosphere for 2 h at room temperature after the first specific-heat measurement, and then it was remeasured again, whereas no change in C_p was found. Other studies on the oxidation of Pd were done by Orent and Bader.[14] They studied the surface of Pd(100) by low-energy electron diffraction and electron energy loss spectroscopy and found only chemisorbed oxygen on the surface at room temperature.

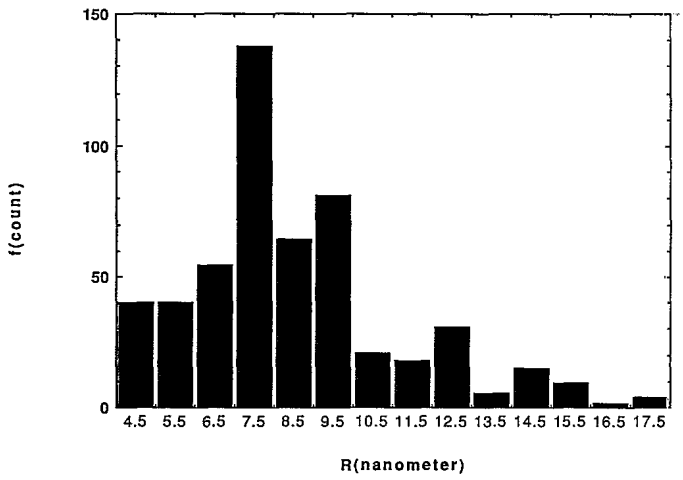

FIG. 1. The distribution of particle sizes observed by transmission electron microscopy.

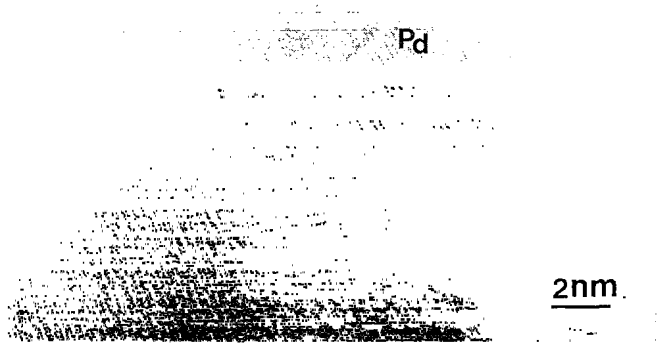

FIG. 2. High-resolution transmission electron microscopy picture showing a Pd nanocrystal in the upper right corner. An internal twin boundary is visible in the nanocrystal.

They did not see PdO until $T\geq200$ °C. A similar result was also observed by Kumar and Saxena.[15] They found the formation of Pd oxides, PdO and Pd_2O, on the vacuum-deposited ultrathin films of Pd at a substrate temperature of 350–400 °C. Although at this stage we cannot rule out the possibility of oxidation on the surface of the nanocrystals, it is believed that the amount of oxidation on the surface should be very small.

Also, in Fig. 2 no disorder or micrograin boundaries are observed, with the exception of a twin boundary. The situation is much simpler than that found in earlier studies[11] of copper nanocrystals, in which micrograins and grain boundaries are believed to be one of the main sources of the extra specific heat, as compared with bulk crystalline copper.

The low-temperature specific-heat measurements were performed using a thermal-relaxation microcalorimeter. The sample, which has two flat sides after compression, was wiped with ~50 microgram of Wakefield grease for good thermal contact and was attached to a sapphire holder on which a germanium thin-film thermometer and a nickel-chromium heater were evaporated. The addenda was then semiaddiabatically isolated from the bath by four gold-copper alloy wires[16] for the thermal-relaxation operation and electrical connections. By recording the time constant τ of the temperature relaxation after switching off the heating power, the specific heat of the specimen can then be measured via $C=k\tau$, where k is the thermal conductance of the link wires. The background of the addenda and grease was properly subtracted, based on a separate measurement. The relative precision and the absolute accuracy of the calorimeter were confirmed to be within ~3% and ~4%, respectively, by measuring a copper standard.

Measurements of the magnetic susceptibility were implemented on the same samples used in specific-heat measurements in a superconducting quantum interference device, which was calibrated with a palladium standard before these measurements. To avoid saturation of the magnetization, a magnetic field scan at 10 K was per-

formed prior to each measurement to determine the proper choice of magnetic field. The x-ray spectra were taken by a rotating-anode x-ray diffractometer made by Material Analysis and Characterization. Before these experiments, a standard silicon powder sample was examined, and the precision of the lattice constant determination was confirmed within 0.03%, which makes it capable of resolving the 0.1% difference of lattice constants observed in this work.

III. EXPECTED CONTRIBUTIONS TO THE SPECIFIC HEAT

In this section we give the expected form[1] for various contributions to the specific heat of nanocrystals: the bulk contribution, that of surface phonons, changes in the bulk electronic contribution due to the quantum size effect, and the surface electronic contribution. The specific heat of an ordinary bulk metal can be represented by the formula

$$C(T)=C_b^e+C_b^p=\gamma_b T+\beta_b T^3 , \tag{1}$$

where

$$\gamma=\frac{nV_m\pi D(\varepsilon_F)K_B^2}{3} \tag{2}$$

and

$$\beta_b=234\frac{NK_B}{\Theta_D^3} . \tag{3}$$

The first term of Eq. (1) is the specific heat of the conduction electrons, and the second term is the specific heat of the lattice phonons. n is the electron density, V_m is the mole volume, $D(\varepsilon_F)$ is the electron density of states at the Fermi level, K_B is the Boltzmann constant, N is the total number of atoms, and Θ_D is the Debye temperature of phonons in the bulk. As mentioned above, due to the higher surface-to-volume ratio and quantum size effects, the thermodynamic properties of nanocrystals are different from those expected for bulk materials. Several new contributions to the specific heat have to be considered in analyzing the specific heat and magnetic susceptibilities of small particles.

A. Enhanced phonon specific heat of small particles

Observation of the enhancement of the specific heat has been reported in many kinds of fine particles, for example 30- and 66-Å palladium particles studied by Comsa, Heitkamp, and Rade,[12] (22–60)-Å lead particles and 22-Å indium particles studied by Novotny and coworkers,[17,18] (29–130)-Å vanadium particles studied by Vergara, Heitkamp, and Lohneysen,[19] and (150–200)-Å aluminum particles and (100–200)-Å silver particles studied by Ohshima, Fujita and Kuroishi.[20] A large portion of the enhancement of specific heat is attributed to surface phonons via a size effect. A model treating small spherical homogeneous particles with free surfaces was provided by Baltes and Hilf.[21] The enhanced specific heat of a small particle is

$$C_p=\sum_l\sum_s\frac{Vm(2l+1)K_Bz^2e^z}{4R^3(e^z-1)^2} \tag{4}$$

with

$$z=\frac{\hbar ca'_{l,s}}{K_BRT} .$$

The maximum $l_{\max}$ satisfies the condition $\sum_1^{l\max}(2l+1)\le N$, where N is the number of atoms contained in a particle, R is the particle radius, V_m is the mole volume and $a'_{l,s}$ is the sth zero of the derivative of the lth spherical Bessel function, and c is the velocity of transverse phonons.

B. Specific heat of bulk conduction electrons

The density of states of conduction electrons in a particle of size d can be described by

$$D(\varepsilon_F)=\frac{d^3}{4\pi^2}\left[\frac{2m}{\hbar^2}\right]^{3/2}\varepsilon^{1/2} . \tag{5}$$

$D(\varepsilon_F)$ is proportional to the volume of the particle, i.e., d^3, and the energy level spacing per spin at the Fermi level will be

$$\delta=\frac{d\varepsilon}{dN}=\frac{4\pi^2}{d^3}\left[\frac{\hbar^2}{2m}\right]^{3/2}\frac{1}{\varepsilon_F^{1/2}} , \tag{6}$$

which is inversely proportional to d^3. For an 84-Å-size Pd nanocrystal, the energy level spacing is about 0.7 K.[1] As long as $\delta/K_B\ll T$, the energy levels of the conduction electrons can be considered to be a continuum, and the specific heat of the bulk electrons is linear in temperature at low T and is represented by

$$C(T)=\gamma_b T . \tag{7}$$

However, for $T\ll\delta/K_B$ the specific heat would be similar to a two-level problem with an energy level spacing δ

$$C_{b,\text{size}}^e=K_B\exp(-\delta/K_BT) . \tag{8}$$

This is a result of the quantum size effect on small particles. The details of the electronic properties of metallic particles is presented by Kubo, Kawabata, and Kobayashi.[22]

C. Specific heat of surface conduction electrons

Because of the lower symmetry at a surface, the band structure on the surface layers is presumed to be different from that of the bulk. So far no measurement of specific heat has been reported that gives direct evidence for this difference, possibly because the difference of the energy band structures between the surface and the bulk is small and easily neglected. The contribution of the surface is[23]

$$C_s^e=\gamma_s T \tag{9}$$

with

$$\gamma_s=\frac{nL^2\pi^2D_s(\varepsilon_F)K_B^2}{3} ,$$

where n is the surface electron density and L^2 is the area of surface. This form is similar to that of the bulk conduction electrons with the bulk density of states replaced by the surface density of states. The details of this contribution will be discussed in the analysis of our specific heat data.

IV. RESULTS AND ANALYSIS

The result for the specific heat of bulk Pd and 84-Å Pd nanocrystals is shown in Fig. 3. The specific heat of bulk Pd is well fit by Eq. (1) with $\gamma_b = 9.7$ mJ/K^2 mol Pd and $\beta_b = 9.5\times10^{-2}$ mJ/K^4 mol Pd; these values are quite consistent with those of Veal and Rayne.[24] The good agreement confirms the performance of our calorimeter. The enhancement of the specific heat can be clearly observed for Pd nanocrystals. The enhancement of the specific heat of 84-Å Pd nanocrystals is about equal to the magnitude estimated from the work of Comsa, Heitkamp, and Rade by extrapolating their results for 30- and 66-Å Pd particles.[12] We observed a decrease of the coefficient of the linear term in Pd nanocrystals, whereas no change was found in the experiments of Comsa, Heitkamp, and Rade. We will return to this point.

The specific heat of small conducting particles is the sum of the contribution of the conduction electrons and of the phonons and can be represented by

$$C = S_f C_s^e + (1-S_f) C_b^e + C^P , \tag{10}$$

where S_f is the surface occupation fraction, C_s^e is the heat capacity of surface conduction electrons represented by Eq. (9), and C_b^e is the heat capacity of bulk conduction electrons. The conduction-electron quantum size effect is negligible for the sizes of 84-Å Pd nanocrystals employed here, given the estimated energy level spacing $\delta = 0.7$ K for 84-Å Pd nanocrystals and the fact that our measurements extend only as low as 0.7 K. In order to see the conduction-electron quantum size effect, T must be much smaller than δ/K_B, so the size of the particle has to be decreased and the temperature of experiment should be lower. Here Eq. (7) is chosen to represent C_b^e, i.e., we assume a continuous distribution of energy levels of the conduction electrons. C^P is represented by the specific heat of small particles using Eq. (4).

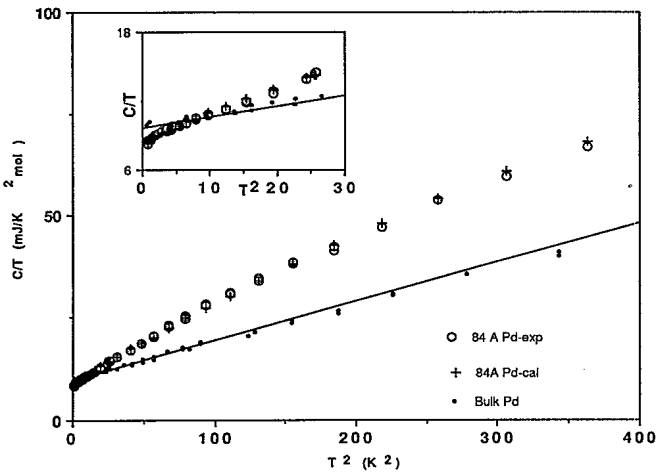

FIG. 3. The specific heat of bulk palladium and 84-Å Pd nanocrystals. The small dots represent bulk Pd and the solid line is its least-squares linear fit. The circles represent the experimental data for the nanocrystals, and the crosses represent the simulation by Eq. (11) with constant velocity of sound $c = 1295$ m/s and linear coefficient of specific heat $\gamma = 7.8\times10^{-3}$ J/K^2 mol (see text). Inset: C/T vs T^2 for data below 5 K.

We fit the data for 84-Å Pd nanocrystals for 0.7 K $< T \leq 20$ K by the following equation derived by substituting Eqs. (4), (7), and (9) into Eq. (10):

$$C_p = \gamma T + \sum_l \sum_s \frac{V_m (2l+1) K_B z^2 e^z}{4R^3 (e^z-1)^2} \tag{11}$$

with

$$z = \frac{\hbar c a'_{l,s}}{K_B R T}$$

and $\gamma = S_f \gamma_s + (1-S_f)\gamma_b$. The result for C/T vs T^2 is plotted in Fig. 3. In fitting the data, the condition $\sum_1^{l\max}(2l+1) = 10900$ for 84-Å Pd nanocrystals is applied, and the coefficient γ and phonon velocity c are kept as adjustable parameters. The values of $\gamma = (7.8\pm0.1)\times10^{-3}$ J/K^2 mol and an average $c \simeq 1295$ m/s are obtained for 84-Å Pd nanocrystals. The magnitude of γ is about 20% smaller than the value 9.7×10^{-3} J/K^2 mol for bulk Pd, which result is different from that observed in the case of small vanadium particles[19] in which the linear coefficient increases with the decrease of particle size. The coefficient of the linear term γ is a sum of γ_b and γ_s. To separate γ_b and γ_s, we assume that the slight softening of the phonons in Pd nanocrystals does not make too much change in the electron-phonon enhancements as compared to that of bulk Pd. Then by taking $\gamma_b = 9.7\times10^{-3}$ J/K^2 mol and accounting for the surface fraction $S_f \simeq 0.28$, which is the ratio of the number of the outer layers atoms to the total number of atoms, the value of the coefficient γ_s is estimated as $\simeq 2.9\times10^{-3}$ mJ/K^2 mol Pd, which is about 30% of the magnitude of γ_b. This indicates a reduction of the density of states at the Fermi level on the surface as compared to the value of the bulk. The coefficients of the fit and the calculated parameters are tabulated in Table I. In the measurements of the magnetic susceptibility of Pd nanocrystals, a similar conclusion is obtained, which will be discussed below. The phonon velocity vs temperature for 84-Å Pd is shown in Fig. 4. For $T < 2$ K a larger scatter in the phonon velocity data is observed; this is due to the less accurate data at low temperatures. However, for $T > 2.2$ K the phonon velocity, which is about 1295 m/s ($\Theta \simeq 226$ K), has an uncertainty of no more than ±50 m/s. The data match quite well to a theoretical simulation by Eq. (11) with the value $c = 1295$ m/s held constant with temperature and $\gamma = 7.8\times10^{-3}$ J/K^2. This comparison is shown in Fig. 3 and in its inset for $T < 5$ K.

TABLE I. The temperature coefficients of the specific heat [Eq. (11)] and the bulk Debye temperatures as derived for bulk and nanocrystals of palladium.

Sample	γ (mJ/K^2 mol)	γ_b (mJ/K^2 mol)	γ_s (mJ/K^2 mol)	c (m/s)	Θ_b (K)
84-Å Pd	7.8±0.1	9.7[a]	2.9	1295	226
Pd bulk	9.7±0.1	9.7		1560	273

[a]Assumed the same as that of the bulk Pd.

This value of c is qualitatively consistent with the result of Comsa, Heitkamp, and Rade. They found that the phonon velocity decreases from 1560 m/s ($\Theta_D=273$ K) for bulk Pd to about 1100 m/s ($\Theta_D=193$ K) and 1000 m/s ($\Theta_D=175$ K) for 66-Å Pd and 30-Å Pd, respectively and for $T<\sim 6$ K. This softening of the phonons, which is dependent on the size of the particle, is the main source of specific-heat enhancement observed in the nanocrystals.

One might suspect that the size effect on the variation of lattice parameters could influence the density of states of the bulk. The x-ray spectra showed, however, that the lattice constants are 3.899 Å and 3.890 Å for 84-Å Pd nanocrystals and bulk palladium, respectively. This slight difference in Pd nanocrystals should have no noticeable effect on the bulk contribution to the specific heat of Pd nanocrystals.

The data for the magnetic susceptibility of bulk palladium and Pd nanocrystals is shown in Fig. 5. The magnitude of the magnetic susceptibility decreases with the decreasing size of the Pd nanocrystals. The magnitude of the magnetic susceptibility is ~70% and ~75% that of the bulk for 84-Å Pd nanocrystals at 150 and 300 K. These values are similar to the net 80% reduction in the specific-heat coefficient, and should have a similar origin. However Ladas, Dalla Betta, and Boudart[8] employed a complicated but convincing technique to measure the surface contribution to the magnetic susceptibility of small Pd particles and found that the surface spin magnetic susceptibility χ_s of small particles was only about 50% and 75% of that of the bulk for temperatures at 150 K and 300 K, respectively. Since the magnetic susceptibility and the temperature coefficient of specific heat are closely related via the electron density of states this confirms our result that $\gamma_s=0.3\gamma_b$ derived from the low temperature specific heat.

In bulk palladium a weak maximum in the magnetic susceptibility is observed near 80 K. A Curie tail observed at $T<20$ K is believed to arise from magnetic impurities: for example, Gerhardt *et al.*[25] measured the magnetic susceptibility in a high-quality palladium sample and found a flat magnetic susceptibility at low temperature. Using the Curie-Weiss relation $\chi=C_{\rm imp}/(T+\theta)+\chi_{\rm Pd}$ to estimate the impurity Curie constant $C_{\rm imp}$ for the bulk and the nanocrystals, we find that the impurity Curie constant for the nanocrystals is about the same as that of the bulk so that the disappearance of the maximum cannot be explained on the basis of an impurity effect.

According to paramagnon theory for an arbitrary band shape, the existence of a peak in $\chi(T)$ can be attributed[26] to a positive coefficient A in the expression

$$\chi(T)=\chi(0)[1+AT^2/(1-\bar{I})^2]\,, \tag{12}$$

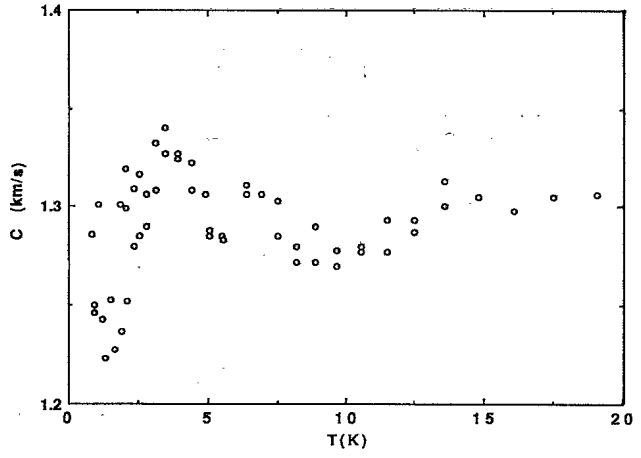

FIG. 4. The phonon velocity vs temperature for 84-Å Pd nanocrystals.

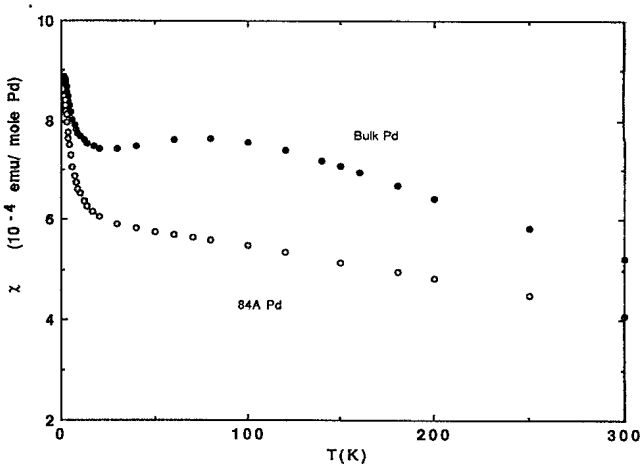

FIG. 5. The magnetic susceptibility of bulk palladium and 84-Å Pd nanocrystals.

where $(1-\bar{I})^{-1}$ is the Stoner enhancement. This coefficient A is a sum of derivatives of the density of states

$$A=[a(N''/N)-b(N'/N)^2]\varepsilon_F \ . \tag{13}$$

The smearing of the peak in χ could then reflect changes in the band structure; for example, $A<0$ for the surface term. It is not possible with the present data to determine directly whether this occurs, but if this argument is true, then the changes in the density of states at the Fermi level must be also reflected in the variation of the coefficients γ of specific heat of the nanocrystals.

V. CONCLUSIONS

We have observed an enhancement of the specific heat in Pd nanocrystals. The enhancement is related both to the softening and the size effect on the phonons. The linear temperature coefficient of specific heat γ decreases to a lower value as compared to that of bulk Pd. This result implies an overall decrease of the electronic density of states at the Fermi level in Pd nanocrystals, and we estimate that the surface density of states is about 30% that of the bulk. This result also corresponds to the measured reduction of the magnetic susceptibility and is qualitatively consistent with the early work of Ladas, Dalla Betta, and Boudart, who found the surface magnetic susceptibility to be about 50% and 75% of that of bulk for temperatures at 150 K and 300 K, respectively. Combined with the disappearance of the peak of magnetic susceptibility at ~80 K in Pd nanocrystals, the energy band structures in Pd nanocrystals must be modified relative to those in bulk. An argument has been pointed out that if a thin layer of oxidation does exit on the surface of a Pd nanocrystal, then the oxide layer with no electronic contribution plus an enhanced electron-phonon interaction, i.e., a larger γ_b for the nanocrystal, would also account for the magnitude of linear coefficient γ. Since the phonon contribution of Pd oxidation is estimated to be larger than that of Pd at the experimental temperatures, a larger phonon contribution to specific heat than that experimentally measured is expected. A compromise to the discrepancy will be that some but not all the surface of the nanocrystal is oxidized.

ACKNOWLEDGMENTS

We would like to thank Professor Jon Lawrence and Professor J. C. Ho for their very helpful discussions and continuing interest and support for our work. This work was supported in part by the National Science Council of the Republic of China under Grant No. NSC82-0208-M-001-148.

[1]W. Halperin, Rev. Mod. Phys. **58**, 533 (1986).
[2]H. E. Schaefer and R. Wurschum, Phys. Lett. A **119**, 370 (1987).
[3]J. Rupp and R. Birringer, Phys. Rev. B **36**, 7888 (1987).
[4]X. Zhu, R. Birringer, U. Herr, and H. Glecter, Phys. Rev. B **35**, 9085 (1987).
[5]R. F. Marzke and W. S. Glaunsinger, Solid State Commun. **18**, 1025 (1976).
[6]C. Suryanarayana and F. H. Froes, Metallurg. Trans. A **23**, 1071 (1992).
[7]R. W. Siegel, Phys. Today **46** (10), 64 (1993).
[8]S. Ladas, R. A. Dalla Betta, and M. Boudart, J. Catalysis **53**, 356 (1978).
[9]J. H. P. Watson, Phys. Rev. **148**, 223 (1966).
[10]C. Y. Lin, K. C. Lee, and Y. D. Yao, Solid State Commun. **83**, 371 (1992).
[11]Y. Y. Chen, Y. D. Yao, B. T. Lin, S. G. Shyu, and H. M. Lin, Chin. J. Phys. **32**, 479 (1994).
[12]G. H. Comsa, D. Heitkamp, and H. S. Rade, Solid State Commun. **24**, 547 (1977).
[13]H. M. Lin (unpublished).
[14]T. W. Orent and S. D. Bader, Surf. Sci. **115**, 323 (1982).
[15]J. Kumar and R. Saxena, J. Less-Common Met. **147**, 59 (1989).
[16]G. M. Schmiedeshoff, N. A. Fortune, J. S. Brooks, and G. R. Stewart, Rev. Sci. Instrum. **58**, 1743 (1987).
[17]V. Novotny, P. P. M. Meincke, and J. H. P. Watson, Phys. Rev. Lett. **28**, 901 (1972).
[18]V. Novotny and P. P. M. Meincke, Phys. Rev. B **8**, 4186 (1973).
[19]O. Vergara, D. Heitkamp, and H. V. Lohneysen, J. Phys. Chem. Solids **45**, 251 (1984).
[20]K. Ohshima, T. Fujita, and T. Kuroishi, J. Phys. Soc. Jpn. **41**, 1234 (1976).
[21]H. P. Baltes and E. R. Hilf, Solid State Commun. **12**, 363 (1973).
[22]R. Kubo, A. Kawabata, and S. Kobayashi, Annu. Rev. Mater. Sci. **14**, 49 (1984).
[23]H. T. Chu, J. Phys. Chem. Solids **49**, 1191 (1988).
[24]B. W. Veal and J. A. Rayne, Phys. Rev. **135**, A442 (1964).
[25]W. Gerhardt, F. Razavi, J. S. Schilling, D. Huser, and J. A. Mydosh, Phys. Rev. B **24**, 6744 (1981).
[26]M. T. Beal-Monod and J. M. Lawrence, Phys. Rev. B **21**, 5400 (1980).